

RSC Advances



This is an *Accepted Manuscript*, which has been through the Royal Society of Chemistry peer review process and has been accepted for publication.

Accepted Manuscripts are published online shortly after acceptance, before technical editing, formatting and proof reading. Using this free service, authors can make their results available to the community, in citable form, before we publish the edited article. This *Accepted Manuscript* will be replaced by the edited, formatted and paginated article as soon as this is available.

You can find more information about *Accepted Manuscripts* in the [Information for Authors](#).

Please note that technical editing may introduce minor changes to the text and/or graphics, which may alter content. The journal's standard [Terms & Conditions](#) and the [Ethical guidelines](#) still apply. In no event shall the Royal Society of Chemistry be held responsible for any errors or omissions in this *Accepted Manuscript* or any consequences arising from the use of any information it contains.

Influence of different membrane environments on the behavior of cholesterol

Zhen-lu Li,^a Jing-jing Wang,^a Hong-ming Ding,^a and Yu-qiang Ma^{*ab}

^a *National Laboratory of Solid State Microstructures and Department of Physics, Nanjing University, Nanjing 210093, China*

^b *Center for Soft Condensed Matter Physics and Interdisciplinary Research, Soochow University, Suzhou 215006, China*

* *E-mail: myqiang@nju.edu.cn*

Abstract

With the aid of molecular dynamics simulations, we study the behavior of cholesterol in several representative membrane environments. Especially, we pay attention to the relation between local lipid packing and the thermodynamic properties of cholesterols in different membranes. It is found that the entropy and enthalpy values of cholesterols in different membranes depend on the membrane lipid packing. Loose lipid packing always corresponds to favorable entropy but disadvantaged enthalpy, while dense lipid packing plays the opposite roles. We further investigate the transbilayer distribution of cholesterols in curved membrane and find that the cholesterol will adjust its distribution in the two leaflets of curved membrane as the two leaflets have different lipid packing style. And quantitatively, we present a simple theory model to explain the redistribution of cholesterols in curved membrane and discuss its potential impact on the membrane deformation process.

I. INTRODUCTION

Cholesterol is an essential and abundant constituent of mammalian cell.^{1,2} It has a wide range distribution in various of organelle membranes as well as the plasma membrane. But the levels of cholesterol can vary greatly among them. For example, it typically accounts for 20-25% of the lipid molecules in the plasma membrane but only as low as 1% of the total cell cholesterol in the endoplasmic reticulum where it is synthesized. The organism has developed sophisticated mechanisms to maintain the lateral and transbilayer distributions of cholesterol in plasma membrane and the overall cellular cholesterol levels among cellular organelles.^{3,4} Disorders in metabolism and transport of the cholesterol can play a key role in some diseases.⁵⁻⁷ For example, excess cholesterol in the cell is associated with atherosclerosis.

Within the class of lipid molecules, the cholesterol is a rather special one. It is combined of a small 3-OH polar headgroup, and a bulky hydrophobic tetrameric ring followed by a short acyl chain. On the whole, it is much more small, rigid and hydrophobic than the other phospholipid components of cell membrane. Hence, it can rigidify the fluid membrane and change the permeability and fluidity of the membrane.⁸⁻¹¹ When mixed with saturated and unsaturated lipids in vitro, it promotes the phase separation of liquid-disordered phase and liquid-ordered phase.¹²⁻¹⁶ Liquid-disordered phase (l_d phase) only has a small quantity of cholesterol, while liquid-ordered phase (l_o phase) is enriched of cholesterol and closely related to the lipid rafts of cellular membrane.¹⁷ In addition, many experiments and simulations have indicated that the cholesterol can flip-flop readily between the two leaflets of membrane,¹⁸⁻²¹ which may help cholesterol adjust itself timely to various of membrane environment. All these unique biophysical properties of cholesterol have made it to be one of the most important regulators of membrane organizations and function. However, the precise mechanism of how cholesterol maintain their specific inter- or intra-membrane distribution and how the specific distribution influences the membrane function is still not well understood. So it is of great importance to do a more detailed investigation on the the interactions between cholesterol and the lipid molecules.

In this work, we will firstly analyze the thermodynamical properties of cholesterol in membrane under serval different conditions and explore some general aspects which can influence the cholesterol behavior. Further simulations will focus on the role of membrane curvature in cholesterol's transbilayer distribution. And a quantitative theory analysis will

be presented to help better understand the transbilayer distribution of cholesterol and its potential influence on the membrane deformation process.

II. METHODS AND MODELS

The MARTINI force field which is developed by Marrink's group^{22,23} is used to perform the molecular dynamics simulations. We mainly construct four different lipid bilayers, i.e., DPPC, DOPC, DPPE and DPPC bilayers under tension. To investigate the condensing effect, they are mixed with cholesterol at different mole fractions from 0% to 60%, with total number of molecules fixed as 256. As an example, Fig. 1A shows a bilayer with 208 DPPC molecules and 48 cholesterol molecules ($\sim 20\%$ cholesterol contents). And the equilibrium configuration of DPPC, DOPC or DPPE bilayer with 20% cholesterol contents can be found in Fig. S1 in the Supporting Information. To calculate free energy for cholesterol partitioning into different pure lipid bilayers, biased simulations are done by using a harmonic potential with a force constant of $1000 \text{ KJ mol}^{-1}\text{nm}^{-2}$ applied between the hydroxyl of cholesterol and the center of mass of bilayer. Each umbrella sampling window includes two cholesterol molecules which are always spaced 4 nm apart along the bilayer normal (Z direction).^{20,24} The first umbrella sampling configuration is shown in Fig. 1B with one cholesterol in the bulk water and the other in the center of bilayer. Consequent 40 configurations are produced by pulling the two cholesterol molecules in the same direction with 0.1 nm per step within the range from $Z = -4.0 \text{ nm}$ to $Z = 4.0 \text{ nm}$. Weighted histogram analysis method (WHAM)²⁵ is applied to calculate the PMF after 480 ns's simulation for each window. To further obtain the entropy and enthalpy contributions, PMFs for three adjacent temperatures (323 K, 333 K, and 343 K) are calculated. By using the centered difference method: $-T\Delta S \approx \frac{T}{2\Delta T}[G(T + \Delta T) - G(T - \Delta T)]$, entropy contribution can be calculated.²⁶ Further, by using the formula $\Delta H = \Delta G + T\Delta S$, the enthalpy contribution can also be estimated. PMFs for DPPC partitioning into pure lipid bilayer is done in the same way, except that the constrain force acts on the phosphate group of DPPC and the simulation time is up to 1280 ns.

To investigate the effect of membrane curvature on the distribution of cholesterol, we push a spherical nanoparticle to an enlarged membrane with a moderate force.²⁷ The enlarged membrane is consisted of 7488 DPPC lipids and 1728 cholesterol molecules (18.8% cholesterol contents). The nanoparticle is constructed by a face-center-cubic lattice consisting of the

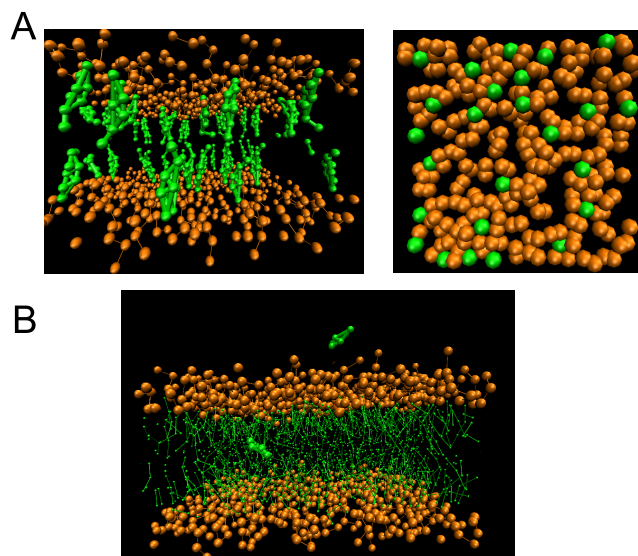


FIG. 1: (A) Configuration of a bilayer with 208 DPPC molecules and 48 cholesterol molecules. Left panel shows the side view of the bilayer including cholesterol molecules and phospholipid headgroup beads and the right panel shows the top view including merely the glycerol ester moiety of the phospholipid and polar hydroxyl group of cholesterol. (B) First umbrella sampling configuration with one cholesterol in the bulk water and the other in the center of bilayer, which is separated by 4 nm in the Z direction. The cholesterol molecule is displayed as big green beads. The phospholipid headgroup is displayed as orange beads and the phospholipid tail is displayed as green thin lines. Water are not shown for clarity.

Martini nonpolar (Nda) beads.²⁸ It is about 10 nm in diameter and moves as a rigid body during the simulation.^{29,30} Standard Martini force field input parameters are used here. Enough water molecules are introduced in all the simulation systems. All simulations are performed in the NPT ensembles with a constant temperature (T) of 323 K and a constant pressure (P) of 1 bar unless otherwise stated. A time step of 20 fs is used for our simulations. Notice that the effective time sampled in CG simulations is 4 times as large as that in atomistic simulations,³¹ so here the effective simulation time step is approximately 80 fs. All simulations and analysis are performed by using GROMACS 4.5.5 software package.³²

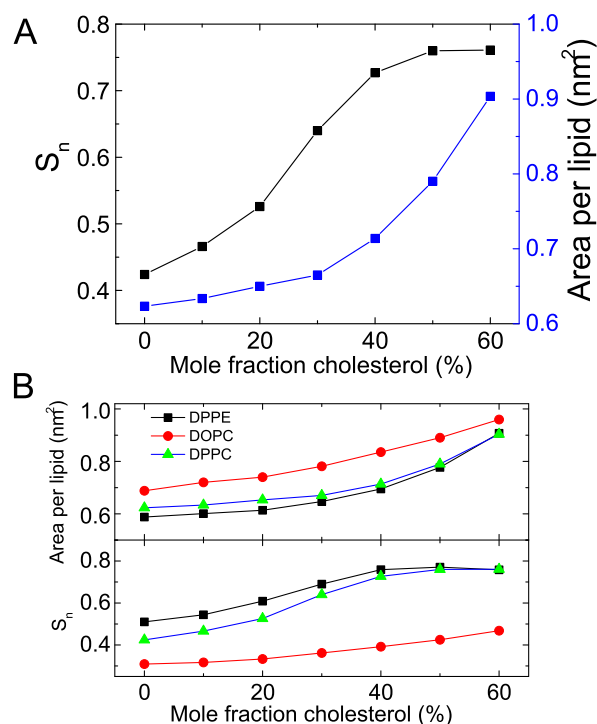


FIG. 2: (A) Profile of order parameter S_n and area per lipid as functions of mole fraction of cholesterol in DPPC bilayer. (B) Contrast among DPPC, DOPC and DPPE bilayers.

III. RESULTS AND DISCUSSION

A. Cholesterol condensing effect

As shown in Fig. 1A, cholesterol molecule locates itself underneath the polar headgroup of phospholipid molecules and its polar hydroxyl group is surrounded by the glycerol ester moiety of the neighboring phospholipid molecules. As it fills the interstitial spaces underneath the of phospholipid headgroup, it can induce the well-known condensing effect^{33–35} (i.e., the averaged cross-sectional area of lipids in the mixed bilayer is reduced). Here, we calculate the acyl chain order parameter S_n and area per lipid as a function of mole fraction of cholesterol (see Fig. 2A). Notice that only the averaged cross-sectional area of DPPC (or DOPC, DPPE) molecules is calculated, namely, the area per lipid is obtained by dividing the total area of membrane by the total number of phospholipid molecules, excluding cholesterol molecules (the area per lipid including cholesterol molecules is shown in Fig. S2 in the Supporting Information). In this way, we can focus on the change of phospholipid's

effective size (mutual interval) upon constantly adding of cholesterol. We find that when the mole fraction of cholesterol is low, S_n has a fast rise while the size of the phospholipid only has a rather small expansion. For example, the area per lipid for pure DPPC bilayer is about 0.625, and the value is about 0.665 for the 30% DPPC bilayer (enlarges about 6%). The 30% DPPC bilayer has 180 DPPC molecules, and we can further imagine that if we add less than 76 cholesterol molecules (30% cholesterol contents) to the pure bilayer of 180 DPPC molecules, the primary lipid bilayer will only has very small expansion which should be less than 6%. So cholesterol has chosen to straighten the acyl chains to better intercalate into the limited space under phospholipid headgroups, instead of enlarging the primary size of phospholipid. This is in accordance with the basic viewpoint of umbrella model that cholesterol needs the protection of phospholipid's polar headgroup.^{36,37} By straightening the acyl tails, the enthalpy will be favorable and some translation entropy may also be obtained as the interstitial space is enlarged, while the configuration entropy of phospholipids is cost. Generally, the whole process should be energetically favorable. In this sense, the whole process resembles like a quasi chemical reaction as the condensed complex model implies.³⁸ However, as the mole fraction of cholesterol increases, the condensing effect will gradually become weak since more and more acyl chains have been straightened, hence the effective size of the phospholipid will enlarge quickly (see Fig. 2A). Starting from the feature of the condensing effect, we can infer that if the type of neighboring lipid varies, the behavior of cholesterol will become different. Take the condensing effect for example, as DOPC has two unsaturated acyl chains which could be more difficult to be straightened, the cholesterol condensing effect in DOPC bilayers is less obvious than that in DPPC and DPPE bilayer (see Fig. 2B). Indeed, the distribution of cholesterol in the DOPC bilayer is relatively disordered. The orientation of cholesterol is more random in the DOPC bilayer, and compared with the case of saturated phospholipid (DPPC, DPPE), there are less polar hydroxyl group of cholesterol residing at the level of glycerol moieties of phospholipid (see Fig. S1). In addition, cholesterol may also influence the lateral distribution of lipid molecules in a multi-component membrane, as recent theory and experiments have shown that lipid of multi-component membrane may tend to adopt regular (superlattice-like) lateral distributions at certain component proportion.^{39,40}

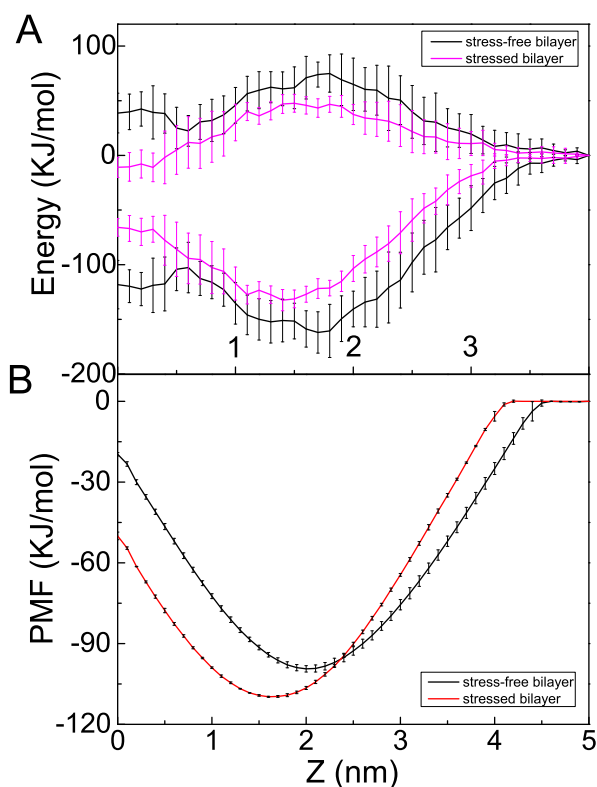


FIG. 3: (A) PMFs for cholesterol partitioning in DPPC bilayers with three different temperature and the corresponding entropy and enthalpy contribution for the PMF of 333K. (B) Entropy and enthalpy contrast between DPPE and DOPC.

B. Thermodynamics analysis of cholesterol in different membranes

As the lipid environment changes, the thermodynamics properties will also change correspondingly. The free energy profile of cholesterol in DPPC bilayer as well as the corresponding entropy and enthalpy components are shown in Fig. 3A. And the curves for DOPC and DPPE bilayers can be found in Fig. S3 of Supporting Information. Major thermodynamic quantities including desorption energy (ΔG_d), entropy ($-T\Delta S$) and enthalpy (ΔH) values around the equilibrium position (z), and free energy barrier (ΔG_b) for moving cholesterol from equilibrium to bilayer center are listed in Table. I. We can find that the desorption energy of cholesterol in three types of lipid membranes only has a small difference, but the values of entropy and enthalpy can be quite different. For example, the difference of entropy value between DOPC and DPPE bilayer is about 45 KJ/mol. As shown in Fig. 3B, entropy

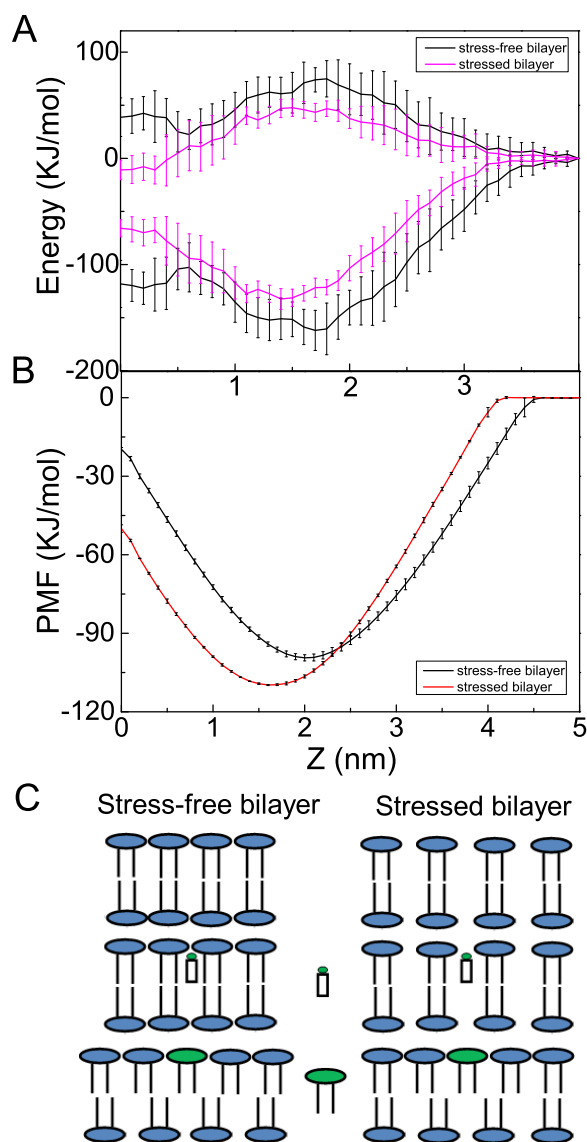


FIG. 4: (A) Entropy and enthalpy contrast between stress-free and stressed DPPC bilayer. (B) PMFs for DPPC partitioning in stress-free and stressed DPPC bilayer. (C) Schematic diagram of adding one cholesterol or phospholipid molecule to the stress-free or stressed bilayer.

and enthalpy contrast curve between DOPC and DPPE bilayer also shows the difference. Since the DOPC bilayer has more loose packing (see Fig. 3B) and the corresponding more free space among phospholipids, cholesterol obtains more entropy in DOPC bilayer. However, the loose packing induces more exposure of nonpolar part of cholesterol with water which yields an unfavorable enthalpy contribution. In contrast, the DPPE bilayer can provide the

best shielding for cholesterol, hence lowest enthalpy value, but the dense packing of DPPE lipid makes the entropy-disadvantaged.

TABLE I: Thermodynamics properties of cholesterol (row 2-5) or DPPC molecule (row 6-7) in different lipid bilayers.

system/condition	z	ΔG_d	ΔG_b	$-T\Delta S$	ΔH
DPPC bilayer	1.5	-91.4	12.2	62.0	-151.5
Stressed bilayer	1.1	-90.6	11.6	40.0	-127.4
DOPC bilayer	1.6	-91.3	9.5	43.2	-130.0
DPPE bilayer	1.5	-95.2	15.5	135.5	-225.2
DPPC bilayer	2.0	-99.3	79.7		
Stressed bilayer	1.6	-109.8	59.8		

To further investigate the influence of phospholipid headgroup on the behavior of cholesterol in the membrane, we directly apply a large lateral (xy-plane) pressure of -50 bar to the DPPC bilayer, and compare the thermodynamics properties of cholesterol in the expanded and stress-free DPPC bilayer (see Fig. 4A and Table. I). Since the size of phospholipid (hence the interstitial spaces) is enlarged under tension, the entropy increases, but the enthalpy is disadvantaged along with more exposure of cholesterol with water. In contrast, we calculate PMFs for a DPPC molecule partitioning into stress-free or stressed DPPC bilayer (see Fig. 4B). It is obvious that the desorption energy for bilayer under tension dramatically decreases compared with the stress-free bilayer. As shown in Fig. 4C, if we add one phospholipid into one leaflet of the stress-free membrane, the whole membrane will expand, or if the total membrane area is fixed, the leaflet with the addition of phospholipid will be much crowded, both of which are energy-disadvantaged. When the phospholipid is added to the stressed membrane, it will fit into the interstitial space and the added phospholipid together with the primary phospholipids will adjust their mutual interval, making it more close to the equilibrium value. In this way, adding one phospholipid can effectively relax the stressed membrane. This could be quite different from that in the case of cholesterol, where low levels of cholesterol inserting into the membrane has little effect on the mutual interval of primary phospholipids. In addition, compared with the case in the stress-free membrane, the cholesterol is more exposed to water in the stressed membrane, which makes it very

enthalpy-disadvantaged. So when facing the stress-free or stressed membrane, the phospholipid will prefer to go into the stressed one to decrease the whole system's free energy, while the cholesterol will have its choice depending on the competitive relation between entropy and enthalpy at specific neighboring environment. On the basis of the above discussion, the cholesterol may not reveal obviously the "stress relaxation effect" asserted in Reference 41, as it can not relax the stressed membrane effectively.

C. Redistribution of cholesterol in curved membrane and discussion on its implication

Besides the types of lipids and the surface tension, the curvature is another principal element which can influence the cholesterol behavior. Actually, the cell experiences various of membrane deformation processes constantly, such as budding, endocytosis, and the vesicular trafficking process.^{2,42-46} It is of great significance to investigate cholesterol's transbilayer distribution when the membrane is deformed. In addition, since the barrier for cholesterol flip-flop is rather small, the easy flip-flop of cholesterol may influence its distribution in the two leaflets. Here, in order to generate a curved membrane, we push a spherical nanoparticle to the membrane with a moderate force. The membrane will adjust its shape constantly until nanoparticle are balanced between the added force and the membrane deformation (see Fig. 5A, and the time sequence of the nanoparticle interacting with the membrane is shown in Fig. S4). Long time simulations (up to 2 μ s) are carried out to observe the distribution and flip-flop of cholesterol. The number of cholesterol in each leaflets are counted; in the meantime, three different portions are distinguished according to the mean curvature: $H \approx 2/R$, $H > 0$ and $H \leq 0$ portion (see Fig. 5A and Table II). More details about partition of the three portions and counting of number of cholesterol molecules can be found in Supporting Information. As shown in Fig. 5A, at the highly curved portion of the membrane, we can find that cholesterol molecules are more "crowded" (enriched) in the inner leaflet (the one closes to the nanoparticle) of the curved membrane. And the detailed counting results (see Table II) show that in $H \approx 2/R$ and $H > 0$ portion, the mole fraction of cholesterol in the inner leaflet is larger than in the outer leaflet, while in the $H \leq 0$ portion, cholesterol is more enriched in the outer leaflet. Both the diffusion and flip-flop of cholesterol can help its redistribution across the bilayer. As shown in Table II,

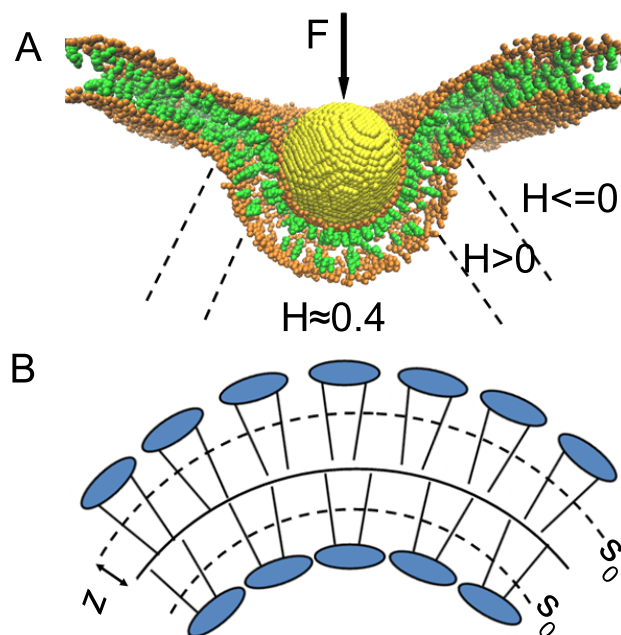


FIG. 5: (A) Final configuration in our simulation. The nanoparticle is in yellow. The phospholipid headgroup is in orange and the cholesterol in green. Water and phospholipid tails are not shown for clarity. Leaflet near the nanoparticle is denoted as “inner leaflet”, and the opposite “outer leaflet”. (B) Schematic diagram of bending the two leaflets of membrane.

more cholesterol molecules go into the inner leaflet through flip-flop in the $H \approx 2/R$, $H > 0$ portion and it is reverse in the $H \leq 0$ portion. When a membrane is curved, the two leaflets are curved independently. As illustrated schematically in Fig. 5B, the headgroup of outer leaflet is stretched a little bit, while the tail portion is compressed. On the contrary, the headgroup of inner leaflet is compressed, but the tail is stretched. On the basis of previous simulation results, we can infer qualitatively that cholesterol can get better protection in the inner leaflet. Thus cholesterol tends to locate in the leaflet where its headgroup size reduces as shown in our simulation (see Table II). Some other experiments and simulations under different conditions also implied the similar distribution characteristics of cholesterol in curved membrane.^{47–50}

To better clarify the redistribution behavior of cholesterol, a quantitative analysis should be helpful. From the above simulation results, we can get the following two points: First, low levels of cholesterol molecules locate themselves underneath the polar headgroup of phospholipid and only have small effect on the primary area of per phospholipid. Hence,

TABLE II: Transbilayer distribution of cholesterol.

	position	$H \approx 2/R$	$H > 0$	$H \leq 0$
CH/DPPC	inner	23/75	89/350	730/3319
	outer	26/185	80/390	781/3169
mole fraction	inner	0.203	0.209	0.180
	outer	0.123	0.170	0.198
headgroup size	inner	0.590		0.675
	outer	0.845		0.652
flip-flop	inner→outer	13		95
	outer→inner	27		75

in a narrow concentration range, we can think that the mutual interval of phospholipid molecules is unchanged upon adding a small quantity of cholesterol molecules. This gives the basis of treating the phospholipid molecules as background. Second, the interactions of cholesterol with the phospholipid molecules in the membrane is closely related to the size of polar phospholipid headgroup (or the averaged mutual interval of phospholipid). Loose lipid packing always corresponds to favorable entropy but disadvantaged enthalpy, while dense lipid packing plays the opposite roles. For example, the area per lipid of the DPPE, DPPC and DOPC bilayer increases in sequence (see Fig. 2B), while the enthalpy of cholesterol in those bilayers increases in sequence (see Table I). What's more, we know that the enthalpy is closely related to the direct intermolecular interaction. Combining the above two points, in a simple way, we can describe the interaction of cholesterol with the phospholipid molecules by a physical quantity ϵ , which denotes the averaged interaction felt by each cholesterol under the action of the neighboring background phospholipid molecules. Based on the area dependency of the enthalpy, we think that ϵ is also dependent on the area of per phospholipid headgroup. In addition, when a membrane is curved, the volume for the two mutual independent monolayer are both incompressible, so much different from the case of stressed membrane, the entropy effect should be small, hence the enthalpy accounts for a major role. Then we can describe the behavior of the cholesterol in the two leaflets just as ideal gas which is divided into two portions: one with external field ϵ_1 , volume V_1 and number of cholesterol molecules N_1 , and the other with ϵ_2 , V_2 and N_2 correspondingly. ϵ is

dependent on the size of the phospholipid headgroup s , which is related to the curvature as $s = s_0(1 \pm zH)$ in the lowest approximation for the two leaflets separately. The total free energy of the two leaflets is expressed as $F/k_B T = N_1 \epsilon_1 + N_2 \epsilon_2 - N_1 \ln(V_1/N_1) - N_2 \ln(V_2/N_2)$. Then we can get the number density ratio (inner/outer) in equilibrium: $\frac{N_1/V_1}{N_2/V_2} = e^{-(\epsilon_1 - \epsilon_2)}$. Common curved membrane domain has diameter of 100 nm to several μm . So the membrane curvature is low, we can consider that the volume (or the phospholipid density on the neutral surface) of the two leaflets is equal ($V_1 = V_2 = V$). Then the redistribution of cholesterol is completely determined by $\frac{N_1}{N_2} = e^{-(\epsilon_1 - \epsilon_2)}$ and the equilibrium free energy is expressed as $F_{equil}/k_B T = N \ln V - N \ln(e^{\epsilon_1} + e^{-\epsilon_2})$, where N is the total numbers of cholesterol. If we further suppose that the area-dependence relation of ϵ can be expanded in series: $\epsilon(s) = \epsilon_0 + \alpha_1(s - s_0) + \alpha_2(s - s_0)^2 + \dots$, we can get $\epsilon_1(H) = \epsilon_0 + \alpha_1 H$ and $\epsilon_2(H) = \epsilon_0 - \alpha_1 H$ by adopting the lowest approximation and using $s = s_0(1 \pm zH)$ (take z as 1 nm). Here, ϵ_0 is for the initial flat membrane. If a local flat membrane is curved into a bud with uniform curvature H (see Fig. 6A), the equilibrium free energy of cholesterol in the curved membrane and the flat membrane will have difference: $\Delta F_{equil}/k_B T = (F_{equil}(H) - F_{equil}(0))/k_B T = -N \ln \frac{\exp(\alpha_1 H) + \exp(-\alpha_1 H)}{2}$. So now we find that the redistribution of cholesterol can help decrease the free energy of the system.

However, we know that a membrane resists elastic deformation, moreover, the membrane including cholesterol has a bigger bending rigidities than the pure phospholipid membrane. Taking the membrane elastic property into account, we continue to consider the membrane deformation process. More explicitly, as shown in Fig. 6A, the l_β domain is surrounded by the bulk l_α domain and it is curved into a bud under the action of line tension (interface energy between the l_α and the l_β domain).⁵¹ The flat membrane domain's area is πL^2 , if it forms a full bud, the bud will have radius $R = \frac{L}{2}$ ($4\pi R^2 = \pi L^2$) and the maximum curvature $H_{max} = \frac{2}{R} = \frac{4}{L}$. Number of cholesterol in the l_β domain is proportional to the membrane area: $N = \frac{2f}{A} \pi L^2$, where f and A denote separately the mole fraction of cholesterol and the area per lipid (including both phospholipid and cholesterol). In the meantime, the total bending energy of the domain is also proportional to the membrane area. So the membrane bending energy E_b and the free energy difference ΔF due to the redistribution of cholesterol can be written together as⁵²: $(E_b + \Delta F)/k_B T = [\frac{1}{2} \kappa H^2 - \frac{2f}{A} \ln \frac{\exp(\alpha_1 H) + \exp(-\alpha_1 H)}{2}] \pi L^2$. Here κ denotes membrane's bending modulus. The line tension energy is expressed as $E_\lambda/k_B T =$

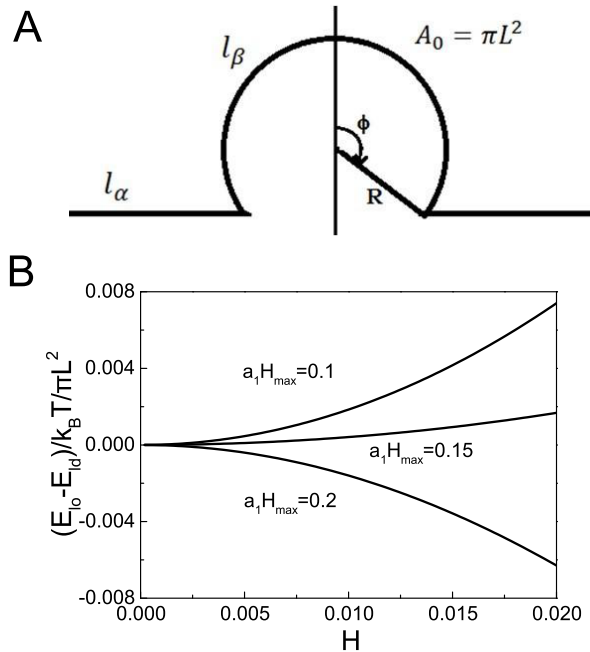


FIG. 6: (A) Schematic diagram of a budding domain. (B) Reduced Energy difference between budding of l_o and l_d domain as function of curvature.

$\lambda 2\pi L[1 - (LH/4)^2]^{\frac{1}{2}}$ with λ denotes the line tension. Then the total energy of system (E_{l_β}) can be written as:

$$E_{l_\beta}/k_B T = \left[\frac{1}{2}\kappa H^2 - \frac{2f}{A} \ln \frac{\exp(\alpha_1 H) + \exp(-\alpha_1 H)}{2} \right] \pi L^2 + \lambda 2\pi L[1 - (LH/4)^2]^{\frac{1}{2}}.$$

So we find that as the redistribution of cholesterol brings an energy decrease of the system, it can help the budding of the domain. If $\alpha_1 H$ is rather small, it seems even explicitly, as the exponential function can be further expanded: $e^{\pm\alpha_1 H} \approx 1 \pm \alpha_1 H + \frac{1}{2}(\alpha_1 H)^2$, then, $\frac{(E_b + \Delta F)/k_B T}{\pi L^2} \approx \frac{1}{2}(\kappa - \frac{2\alpha_1^2 f}{A})H^2 = \frac{1}{2}\kappa_{eff}H^2$. It can be seen that the effective bending modulus decreases due to the redistribution of cholesterol, which consists with the results by using molecular theory.⁵³ If higher order terms of the series $\epsilon(H)$ are considered, κ_{eff} will be also dependent on H or H^2 . It reminds us of the work done by Müller etc.,⁵⁰ where they used a curvature dependent bending modulus: $\kappa_{eff} = \kappa(1 - (dH)^2)$. Other cases when $\alpha_1 H$ is not very small are discussed in Supporting Information. Besides, another interesting thing deserved to be considered is related to budding phenomenon of liquid-order l_o phase and liquid-disorder l_d phase. Since the l_o domain has a rather big bending modulus, it should be

unfavorable for budding in most cases. But in certain experiment conditions, the budding of l_o phase rather than l_d phase is observed.^{54,55} Considering that l_o domain has more cholesterol than the l_d domain, the redistribution of cholesterol in curved membrane should be more prominent, as the redistribution of cholesterol can help decrease the free energy energy of the system, it may help the budding of l_o domain. We can compare the energy difference of budding a l_o and l_d domain: $\frac{(E_{l_o}-E_{l_d})/k_B T}{\pi L^2} = \frac{1}{2}(\kappa_{l_o} - \kappa_{l_d})H^2 - 2\left(\frac{f_{l_o}}{A_{l_o}} - \frac{f_{l_d}}{A_{l_d}}\right) \ln \frac{\exp(\alpha_1 H) + \exp(-\alpha_1 H)}{2}$ (Note that line tension energy E_λ is cancelled out). Considering of a domain with $L=200$ nm and taking representative value of bending modulus and mole fraction of cholesterol for the two domain: $\kappa_{l_d} = 15$, $f_{l_d} = 0.1$ and $\kappa_{l_o} = 75$, $f_{l_o} = 0.4$. Area per lipid can be obtained from the molecular dynamics simulation: $A_{l_o} = 0.423$ and $A_{l_d} = 0.574$. Then the energy difference is drawn as the function of membrane curvature H (state with certain budding extent), which is shown in Fig. 6B. We can find that along with the enlargement of $\alpha_1 H_{max}$, the energy difference constantly decreases from positive value to negative value. So, generally, l_d domain is easier to be curved, however, if $\alpha_1 H$ is large enough, the redistribution of cholesterol may make the budding of l_o phase more favorable than that of l_d phase. In addition, it should be noted that the redistribution of cholesterol will induce the change of mole fraction of cholesterol in each leaflets. In turn, the change of mole fraction of cholesterol will influence the phospholipid's size. We have omitted this effect in the above discussion, but as the membrane curvature is low, the area change of phospholipid headgroup induced by membrane bending ($s = s_0(1 \pm zH)$) is small as well. So a careful analysis of this effect should be investigated, which is also presented in the additional discussion section in the Supporting Information. Overall, the discussion here is only primary, but still it shows that the redistribution of cholesterol upon the two leaflets of membrane can help decrease the energy cost of membrane bending, and in certain conditions this mechanism may even make the more rigid membrane easier to be curved than the less rigid membrane.

IV. CONCLUSION

In the present paper, we have investigated the behavior of cholesterol in several representative membrane environments. It is found that different membrane lipid packing can change the thermodynamics properties of cholesterol in different membrane environments, which will in turn influence the inter- or intra-membrane distribution of cholesterol. In

particular, we find that loose lipid packing always corresponds to favorable entropy but disadvantaged enthalpy, while dense lipid packing plays the opposite roles. Besides, we investigate the distribution of cholesterol in the two leaflets of curved membrane and point out that the redistribution of cholesterol can help decrease the energy cost of membrane bending. This work can help better understand the specific inter- or intra-membrane distribution behavior of cholesterol. In the meantime, it sheds some light on the potential implication of the redistribution of cholesterol.

Acknowledgment: This work is supported by the National Natural Science Foundation of China (No. 91027040) and the National Basic Research Program of China (No. 2012CB821500). We are grateful to the High Performance Computing Center (HPCC) of Nanjing University for doing the numerical calculations in this paper on its IBM Blade cluster system.

-
- ¹ G. van Meer, D. R. Voelker and G. W. Feigenson, *Nat. Rev. Mol. Cell. Bio.*, 2008, **9**, 112.
 - ² E. Ikonen, *Nat. Rev. Mol. Cell. Bio.*, 2008, **9**, 125.
 - ³ K. Simon and E. Ikonen, *Science*, 2000, **290**, 1721.
 - ⁴ F. R. Maxfield and A. K. Menon, *Curr. Opin. Cell Biol.*, 2006, **18**, 379.
 - ⁵ F. R. Maxfield and I. Tabas, *Nature*, 2005, **438**, 612.
 - ⁶ P. Linsel-Nitschenke and A. R. Tall, *Nat. Rev. Drug Discovery*, 2005, **4**, 193
 - ⁷ E. Ikonen, *Physiol. Rev.*, 2006, **86**, 1237.
 - ⁸ F. de Meyer and B. Smit, *Proc. Natl. Acad. Sci. U. S. A.*, 2009, **106**, 3654.
 - ⁹ J. Pan and T. T. Mills, S. T. Nagel and J. Nagle, *Phys. Rev. Lett.*, 2008, **100**, 198103.
 - ¹⁰ N. Khatizadeh, S. Gupta, B. Farrell, W. E. Brownell and B. Anvari, *Soft Matter*, 2012, **8**, 8350.
 - ¹¹ M. E. Solmaz, S. Sankhagowit, R. Biswas, C. A. Mejia, M. L. Povinelli and N. Malmstadt, *RSC Adv.*, 2013, **3**, 16632.
 - ¹² S. L. Veatch and S. L. Keller, *Phys. Rev. Lett.*, 2002, **89**, 268101.
 - ¹³ T. Baumgart, S. T. Hess and W. W. Webb, *Nature*, 2003, **425**, 821.
 - ¹⁴ R. Elliott, I. Szleifer and M. Schick, *Phys. Rev. Lett.*, 2006, **96**, 098101.
 - ¹⁵ H. J. Risselada and S. J. Marrink, *Proc. Natl. Acad. Sci. U. S. A.*, 2008, **105**, 17367.
 - ¹⁶ C. L. Armstrong, W. Haubler, T. Seydel, J. Katsaras and M. C. Rheinstadter, *Soft Matter*,

- 2014, **10**, 2600.
- ¹⁷ K. Simons and E. Ikonen, *Nature*, 1997, **387**, 569.
- ¹⁸ K. John, J. Kubelt, P. Muller, D. Wustner and A. Herrmann, *Biophys J.*, 2002, **83**, 1525.
- ¹⁹ T. L. Steck and J. Ye and Y. Lange, *Biophys J.*, 2002, **83**, 2118.
- ²⁰ W. F. D. Bennett, J. L. MacCallum, M. J. Hinner, S. J. Marrink and D. P. Tieleman, *J. Am. Chem. Soc.*, 2009, **131**, 12714.
- ²¹ G. Parisio, M. M. Sperotto and A. Ferraini, *J. Am. Chem. Soc.*, 2012, **134**, 12198.
- ²² S. J. Marrink, H. J. Risselada, S. Yefimov, D. P. Tieleman and A. H. de Vries, *J. Phys. Chem. B*, 2007, **111**, 7812.
- ²³ S. J. Marrink and D. P. Tieleman, *Chem. Soc. Rev.*, 2013, **42**, 6801.
- ²⁴ W. F. D. Bennett, J. L. MacCallum, and D. P. Tieleman, *J. Am. Chem. Soc.*, 2009, **131**, 1972.
- ²⁵ B. Roux, *Comput. Phys. Commun.*, 1995, **91**, 275.
- ²⁶ J. L. MacCallum, and D. P. Tieleman, *J. Am. Chem. Soc.*, 2006, **128**, 125.
- ²⁷ K. Yang and Y. Q. Ma, *Nat. Nanotechnol.*, 2010, **5**, 579.
- ²⁸ Z. L. Li, H. M. Ding and Y. Q. Ma, *Soft Matter*, 2013, **9**, 1281.
- ²⁹ H. M. Ding, W. D. Tian and Y. Q. Ma, *ACS Nano*, 2012, **6**, 1230.
- ³⁰ H. M. Ding and Y. Q. Ma, *Sci. Rep.*, 2013, **3**, 2804.
- ³¹ S. J. Marrink, A. H. de Vries and A. E. Mark, *J. Phys. Chem. B*, 2004, **108**, 750.
- ³² D. V. D. Spoel, E. Lindahl, B. Hess, G. Groenhof, A. E. Mark and H. J. C. Berendsen, *J. Comput. Chem.*, 2005, **26**, 1701.
- ³³ T. P. W. McMullen, R. N. A. H. Lewis and R. N. McElhaney, *Curr. Opin. Colloid Interf. Sci.*, 2004, **8**, 459.
- ³⁴ C. Hofsbab, E. Lindahl and O. Edholm, *Biophys. J.*, 2003, **84**, 2192.
- ³⁵ O. Edholm and J. F. Nagel, *Biophys. J.*, 2005, **89**, 1827.
- ³⁶ J. Huang and G. W. Feigenson, *Biophys J.*, 1999, **76**, 2142.
- ³⁷ M. R. Ali, K. H. Cheng and J. Huang, *Proc. Natl. Acad. Sci. U. S. A.*, 2007, **104**, 5372.
- ³⁸ A. Radhakrishnan and H. McConnel, *Proc. Natl. Acad. Sci. U. S. A.*, 2005, **102**, 1262.
- ³⁹ P. Somerharju, J. A. Virtanen, K. H. Cheng and M. Hermansson, *BBA-Biomembr.*, 2009, **1788**, 12.
- ⁴⁰ B. Cannon, A. Lewis, P. Somerharju, J. Virtanen, J. Huang, and K. H. Cheng, *J. Phys. Chem. B*, 2010, **114**, 10105.

- ⁴¹ R. J. Bruckner, S. S. Mansy, A. Ricardo, L. Mahadevan and J. W. Szostak, *Biophys J.*, 2009, **97**, 3113.
- ⁴² U. Seifert, *Adv. Phys.*, 1997, **46**, 13.
- ⁴³ P. B. S. Kumar, G. Gompper and R. Lipowsky, *Phys. Rev. Lett.*, 2001, **86**, 3911.
- ⁴⁴ M. Deserno, *Phys. Rev. E*, 2004, **69**, 031903.
- ⁴⁵ H. T. McMahon and J. L. Gallop, *Nature*, 2005, **438**, 590.
- ⁴⁶ I. Canton and G. Battaglia, *Chem. Soc. Rev.*, 2012, **41**, 2718.
- ⁴⁷ W. C. Wang, L. Yang, and H. W. Huang, *Biophys J.*, 2007, **92**, 2819.
- ⁴⁸ H. Lee, H. R. Kim, R. G. Larson and J. C. Park, *Macromolecules*, 2012, **45**, 7304.
- ⁴⁹ S. O. Yesylevskyy and A. P. Demchenko, *Eur Biophys J*, 2012, **41**, 1043.
- ⁵⁰ H. J. Risselada, S. J. Marrink and M. Muller, *Phys. Rev. Lett.*, 2011, **106**, 148102.
- ⁵¹ R. Lipowsky, *J. Phys. II France*, 1992, **2**, 1825.
- ⁵² W. Helfrich, *Z. Naturforsch. C*, 1973, **28**, 693.
- ⁵³ M. J. Uline and I. Szleifer, *Faraday Discuss.*, 2013, **161**, 177.
- ⁵⁴ K. Bacia, P. Schwille and T. Kurzchalia, *Proc. Natl. Acad. Sci. U. S. A.*, 2005, **102**, 3272.
- ⁵⁵ M. Yanagisawa, M. Imai and T. Taniguchi, *Phys. Rev. Lett.*, 2008, **100**, 148102.

For Table of Contents Use Only

Zhen-lu Li, Jing-jing Wang, Hong-ming Ding, Yu-qiang Ma

Influence of different membrane environments on the behavior of cholesterol

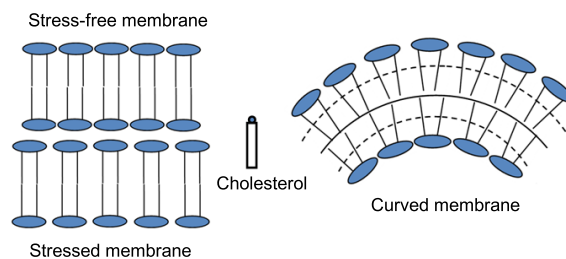


FIG. 7: Our results show the distribution of cholesterol between stress-free and stressed membrane or between the inner leaflet and the outer leaflet of curved membrane.